

1 **Supplemental Information**

2

3 **Supplemental Materials and Methods**

4 **Gene expression analysis**

5 The National Institutes of Gene Expression Omnibus (GEO) database was used to  
6 obtain gene expression data in all kinds of cancers  
7 (<https://www.ncbi.nlm.nih.gov/geo/>). The probe set ID of APOBEC3B in kidney  
8 cancer (GSE66270), cervical cancer (GSE63514), non-small cell lung cancer  
9 (GSE27262) and hepatocellular carcinoma (GSE14520) was 206632\_s\_at. The probe  
10 set ID of APOBEC3B in head and neck squamous cell cancer (GSE58911) was  
11 8073062. The probe set ID of APOBEC3B in ovarian cancer (GSE12470) was 22344.  
12 The probe set ID of APOBEC3B in bladder cancer (GSE37815) was ILMN\_1691457.  
13 The probe set ID of APOBEC3B in breast cancer (GSE109169) was 3945545. The  
14 probe set ID of APOBEC3B in anaplastic thyroid cancer (GSE65144) was  
15 206632\_s\_at. The probe set ID of APOBEC3B in papillary thyroid cancer (GSE50901)  
16 was 24480. The probe set ID of APOBEC3B and PD-L1 (CD274) in ESCC  
17 (GSE17351) and colon cancer (GSE606970) were 206632\_s\_at and 227458\_at,  
18 respectively. The probe set ID of APOBEC3B, PD-1 and PD-L1 (CD274) in Renal  
19 cell carcinoma (GSE67501) and Melanoma (GSE79691) were ILMN\_2219466,  
20 ILMN\_1806725 and ILMN\_1701914, respectively. The probe set ID of mouse  
21 APOBEC3 and mouse PD-L1 (CD274) in AOM/DSS induced colon cancer were  
22 A\_65\_P17700 and A\_51\_P248666, respectively.

23

## 24 **Cell lines**

25 Human esophageal squamous cell carcinoma cell lines (KYSE70, KYSE150),  
26 human colon cancer cell line (RKO), human umbilical vein endothelial cell line  
27 (HUVEC) and immortalized normal esophageal cell line (HET-1A) were cultured in  
28 Roswell Park Memorial Institute (RPMI) 1640 complete medium (Gibco, Grand  
29 Island, USA) supplemented with 10% fetal bovine serum (FBS, BI, USA), 100 U/mL  
30 penicillin (Solarbio, China) and 100 µg/mL streptomycin (Solarbio, China). Human  
31 embryonic kidney cell line (HEK-293T) was cultured in Dulbecco Modified Eagle  
32 Medium (DMEM) (Gibco, Grand Island, USA) supplemented with 10% FBS, 100  
33 µg/mL streptomycin and 100 U/mL penicillin. All cells were incubated in a sterile  
34 incubator with 5% CO<sub>2</sub> at 37°C.

35

## 36 **Plasmid construction and transfection**

37 The full-length nucleic acid sequence of APOBEC3B was optimized by Shanghai  
38 Ziben Biotechnology Co., Ltd (Shanghai, China) and cloned into pLVX-Tetone-GP3  
39 vector through *Age* I and *Not* I restriction sites. Subsequently, APOBEC3B  
40 overexpression vector and empty vector were transfected into KYSE150 cells with  
41 PowerTrans 293 (Sixiang Biological, SX-TR293-001, China) according to the  
42 protocol. Finally, KYSE150 cells overexpressing APOBEC3B were induced by  
43 doxycycline (dox).

44

## 45 **Western blot**

46 The total cell lysates were prepared using protein lysis buffer. Then protein was

47 fractionated by 8% SDS PAGE, transferred to polyvinylidene fluoride (PVDF)  
48 membrane (Merck Millipore, IPVH00010, USA), and then blocked with 5% defatted  
49 milk dissolved in PBS (pH7.2) containing 0.1% Tween 20 for 2 hours at room  
50 temperature. The PVDF membranes were incubated with antibody of human  
51 APOBEC3B (Abcam, ab184990, UK) overnight at 4 °C. The reference antibody was  
52 GAPDH (Servicebio, GB11002, China). After incubation of PVDF membranes with  
53 secondary antibody (Sangon Biotech, D110011-0100, China), the blots were  
54 visualized using ECL system (Azure C600, USA).

55

#### 56 **Cell viability assay**

57 Effect of compounds on the proliferation of cells were determined by MTT assay.  
58 Briefly, KYSE70, HEK-293T, HUVEC and HET-1A cells were seeded into 96 plates  
59 (3000 cells/well) and grew overnight. Cells were then synchronized by starvation with  
60 serum-free RPMI 1640 medium or DMEM for 8 hours, followed by treating with  
61 different concentrations of compounds in complete medium for 24 hours, 48 hours  
62 and 72 hours, respectively. MTT (Sigma, USA) dissolved in PBS were then added and  
63 cultured for 4 hours at 37°C. Formazan crystals formed by viable cells were dissolved  
64 by 150 µL of DMSO, and the absorbance was measured by using a multi-functional  
65 microplate detector at 490 nm. Cell viability was calculated as the formula:

$$66 \text{ Cell viability (\%)} = (\text{OD}_{\text{Experimental group}} - \text{OD}_{\text{Blank group}}) / (\text{OD}_{\text{Ctrl group}} - \text{OD}_{\text{Blank group}}) \\ 67 \times 100\%$$

68

#### 69 **Microscale Thermophoresis (MST) assay**

70 The detailed method was described in materials and methods in the main text. The

71 experimental concentration of APOBEC3A protein (MedChemExpress, HY-P72080,  
72 USA) was 5  $\mu$ M. The experimental concentration of APOBEC3G protein (Abnova,  
73 H00060489-P01, China) was 3  $\mu$ M.

74

#### 75 **Fluorescence-based single-stranded DNA cytosine deamination assay**

76 The detailed method was described in materials and methods in the main text. The  
77 final reaction concentration of APOBEC3A and APOBEC3G was 0.4  $\mu$ M.

78

#### 79 **H&E staining and Immunofluorescence analysis**

80 The APOBEC3B antibody in immunofluorescence analysis was purchased from the  
81 Absin Bioscience Inc. (Shanghai, China), and the dilution ratio was 1:100 for  
82 immunofluorescence analysis. The H&E staining and immunofluorescence analysis  
83 were accomplished by the Wuhan Service Biotechnology company in China.

84

#### 85 ***In vivo* toxicity analysis**

86 The fresh whole blood was taken from mice, quickly added to the buffer containing  
87 heparin sodium, and then sent to the laboratory department of hospital for blood  
88 routine analysis containing WBC, RBC, HGB, PLT and so on. The serum was  
89 collected for blood biochemistry (AST and ALT) analysis according to the protocol.

90

#### 91 **T cell migration assay**

92 The chemotaxis of CD8<sup>+</sup> T cells was measured by transwell assay. The aperture of

93 chamber (Corning, 3421, USA) was 0.5  $\mu\text{m}$ . The peripheral blood mononuclear cells  
94 (PBMCs) from human donors were isolated and activated with 100 units IL-2, 1  
95  $\mu\text{g}/\text{mL}$  anti-CD3, and 1  $\mu\text{g}/\text{mL}$  anti-CD28 stimulatory antibodies for 2 days. Then,  
96 activated PBMCs were harvested, centrifuged and resuspended in serum-free RPMI  
97 1640 medium. 200  $\mu\text{L}$  PBMCs suspensions ( $1 \times 10^5$  cells) were seeded into the upper  
98 chamber. Then, 600  $\mu\text{L}$  RPMI 1640 complete medium, supernatant of KYSE70  
99 (vehicle group) and supernatant of KYSE70 pretreated with 10  $\mu\text{M}$  3,  
100 5-diiodotyrosine for 48 hours were added into the lower chamber, respectively. Three  
101 days later, the migration number of  $\text{CD8}^+$  T cells was analyzed by flow cytometry.

102

#### 103 **Assessment of disease activity index in colon cancer mice model**

104 The disease activity index (DAI) of mice was assessed based on changes in body  
105 weight (such as whether body weight increased or decreased), appearance of stool,  
106 and hematochezia of stool.

107

108

109

110

111

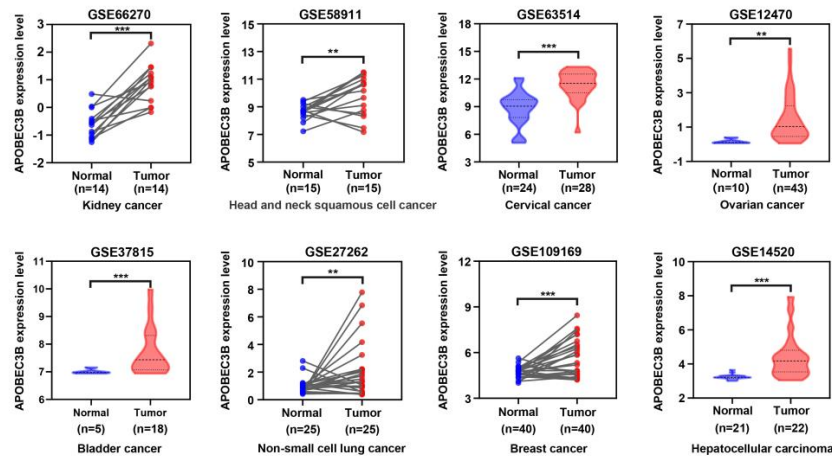
112

113

114

115

116

117 **Supplementary Figures and Tables**

118

119 **Figure S1.** The expression level of APOBEC3B in normal and tumor tissues of  
 120 different cancer types from GEO database. Data from GEO database have performed  
 121 background correction and normalization. The statistical analysis was performed by  
 122 one-tailed Student's *t* test (\*\* $P < 0.01$ , \*\*\* $P < 0.001$ ).

123

124

125

126

127

128

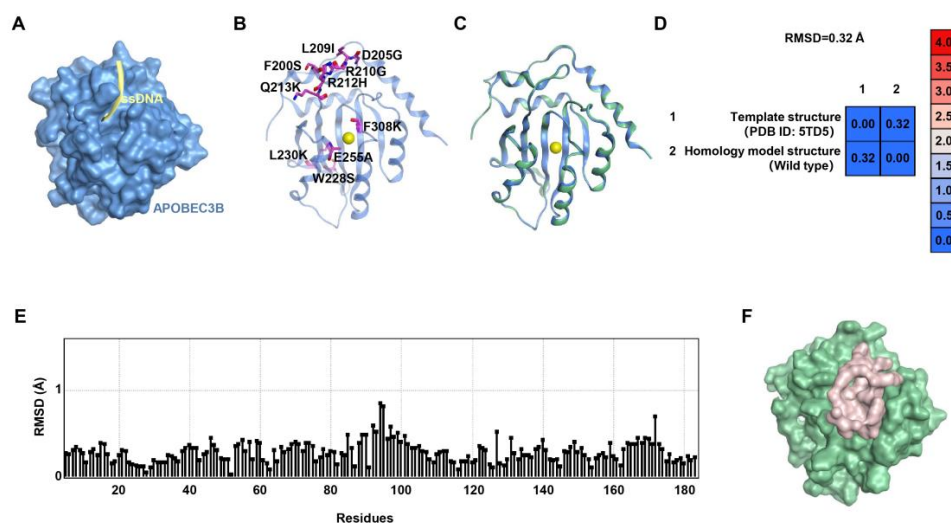
129

130

131

132

133



134

135 **Figure S2.** The structure of APOBEC3B. (A) The reported X-ray cocrystal structure

136 of APOBEC3B (blue) with its substrate ssDNA (yellow) from PDB (PDB ID: 5TD5).

137 (B) The mutated sites (purple) of APOBEC3B in cocrystal structure. The yellow dot

138 showed the zinc ion in APOBEC3B structure. (C, D) The homology model structure

139 (wild type, green) was superimposed with template structure (blue) with an RMSD of

140 0.32 Å by MOE. (E) The all-residue RMSD of homology model structure compared

141 to template structure. (F) The pocket surface (pink) of wild type APOBEC3B suitable

142 for screening compounds.

143

144

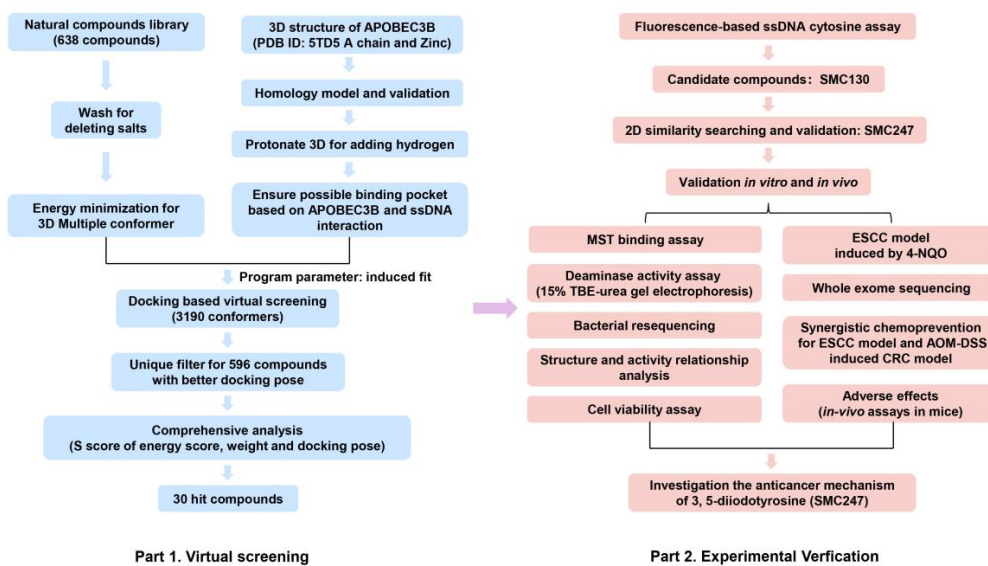
145

146

147

148





149

150 **Figure S3.** The comprehensive workflow chart in this research. The blue part on the

151 left was virtual screening process using computer, and the pink part on the right was

152 experimental verification process.

153

154

155

156

157

158

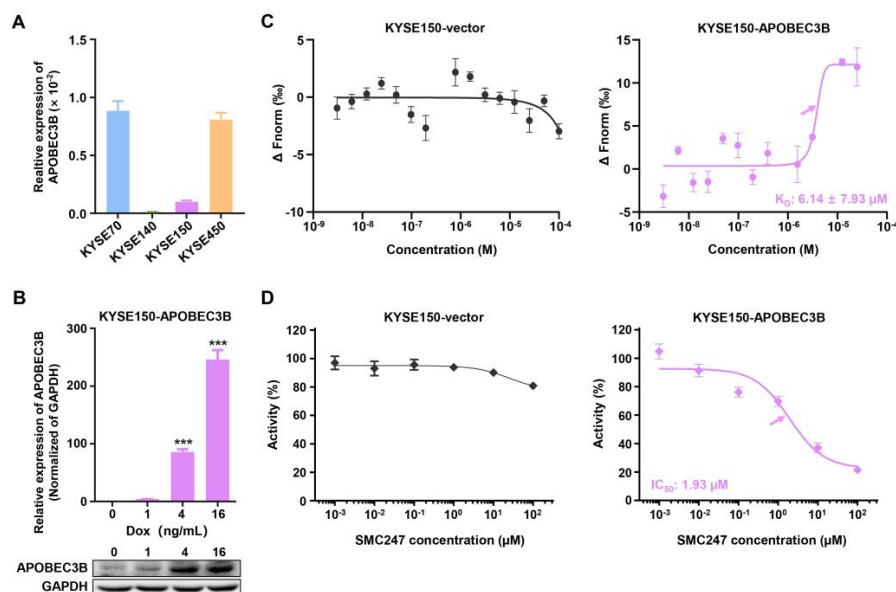
159

160

161

162

163



164

165 **Figure S4.** The interaction between 3, 5-diiodotyrosine and APOBEC3B in cancer

166 cells. (A) The mRNA expression level of APOBEC3B in different ESCC cell lines.

167 GAPDH was considered as the reference gene. (B) The mRNA and protein expression

168 levels of APOBEC3B after KYSE150 cells were transfected with expression vector

169 and induced by different concentrations of doxycycline (dox). (C, D) The interaction

170 between 3, 5-diiodotyrosine and APOBEC3B were measured within KYSE150-vector

171 (Empty vector was stably expressed in KYSE150 cells) and KYSE150-APOBEC3B

172 (APOBEC3B vector was stably expressed in KYSE150 cells) cells by MST and

173 fluorescence-based ssDNA deaminase analysis. Arrows showed the  $K_D$  or  $IC_{50}$ 

174 concentration values. Data are representative of at least three independent

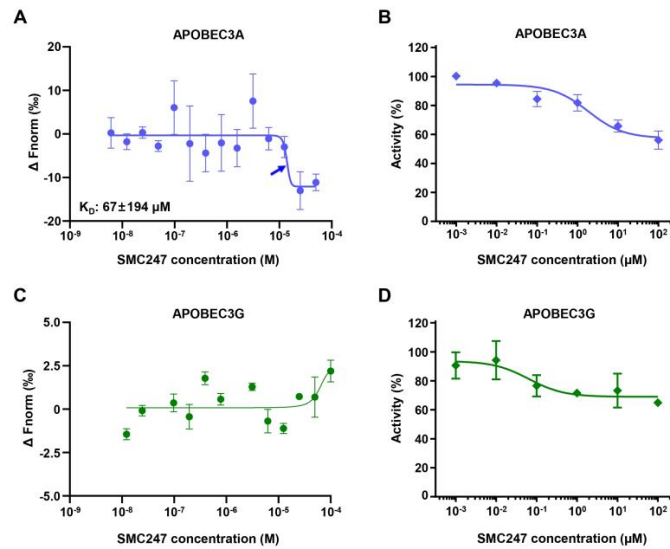
175 experiments.

176

177

178





180

181 **Figure S5.** The interaction of 3, 5-diiodotyrosine with APOBEC3A and APOBEC3G.

182 (A) The curves of 3, 5-diiodotyrosine binding to human APOBEC3A protein and

183 APOBEC3G protein. (B) The curves of 3, 5-diiodotyrosine affecting on APOBEC3A

184 and APOBEC3G deaminase activity. Arrows showed the  $K_D$  or  $IC_{50}$  concentration185 values. The absence of label indicated that  $K_D$  or  $IC_{50}$  could not be fitted. The data are

186 representative of at least three independent experiments.

187

188

189

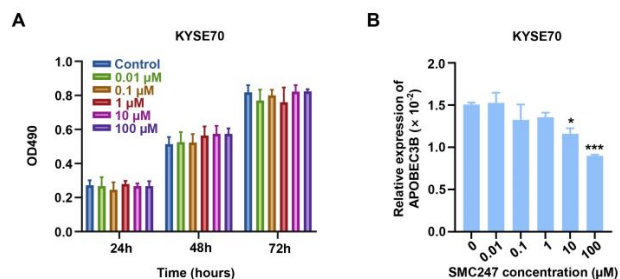
190

191

192

193

194



195

196 **Figure S6.** The effects of 3, 5-diiodotyrosine on the proliferation of KYSE70 cell and

197 expression level of APOBEC3B. (A) Effects of different concentrations (0, 0.01, 0.1,

198 1, 10, 100  $\mu\text{M}$ ) of 3, 5-diiodotyrosine on the proliferation of KYSE70 tumor cell were

199 measured by MTT. (B) The mRNA expression levels of APOBEC3B after 3,

200 5-diiodotyrosine treatment. KYSE70 cells with high expression of APOBEC3B were

201 treated with different concentrations (0, 0.01, 0.1, 1, 10 and 100  $\mu\text{M}$ ) of 3,

202 5-diiodotyrosine for 48 hours, and then the mRNA expression levels of APOBEC3B

203 were measured by qRT-PCR. (Mean  $\pm$  SD were shown for triplicate reactions204 normalized to GAPDH, \* $P < 0.05$  and \*\*\* $P < 0.001$  by two-tailed Student's t test).

205 Data are representative of at least three independent experiments.

206

207

208

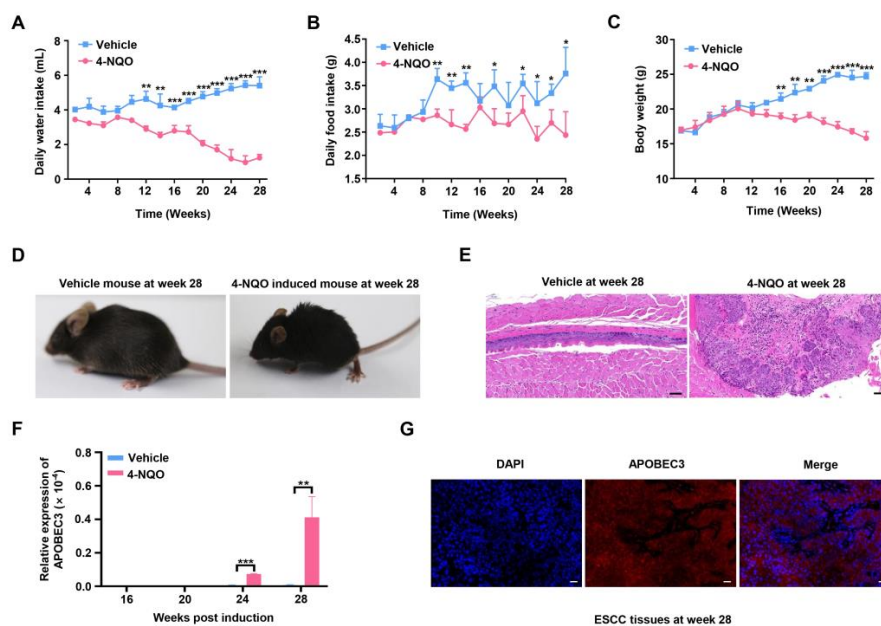
209

210

211

212

213



214

215 **Figure S7.** Model establishment and physiological indexes of 4-NQO induced ESCC

216 mice. (A) Water intake, (B) Food intake and (C) body weight of vehicle mice and

217 4-NQO induced ESCC mice (\* $P < 0.05$ , \*\* $P < 0.01$  and \*\*\* $P < 0.001$  by two-tailed218 Student's  $t$  test). (D) Representative physiological state images of vehicle mice and

219 4-NQO induced C57BL/6J mice at 28th weeks. (E) Histopathological condition of

220 vehicle and 4-NQO induced mice at 28 weeks was determined by H&amp;E staining assay

221 (Scale bars: 50  $\mu\text{m}$ ). (F) The mRNA expression level of APOBEC3 was detected in

222 esophagus tissues of vehicle and 4-NQO induced ESCC mice at different periods

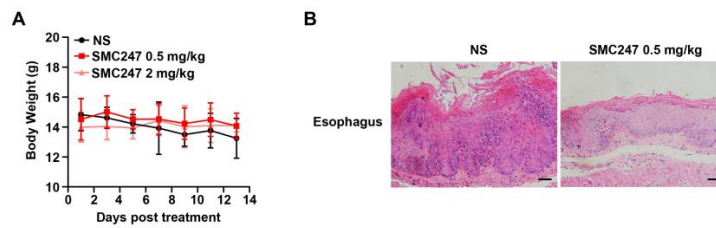
223 (\*\* $P < 0.01$ , \*\*\* $P < 0.001$ ). (G) Protein expression of APOBEC3 in esophagus

224 tissues of 4-NQO induced ESCC mice at week 28 was detected by

225 immunofluorescence analysis (Scale bars: 20  $\mu\text{m}$ ).

226

227



228

229 **Figure S8.** The physiological assessment of mice. (A) Body weight changes of mice

230 (n = 5). (B) Histopathological assessment of esophagus tissues in NS and 3,

231 5-diiodotyrosine groups were determined by H&amp;E staining assay (Scale bars: 100

232  $\mu\text{m}$ ).

233

234

235

236

237

238

239

240

241

242

243

244

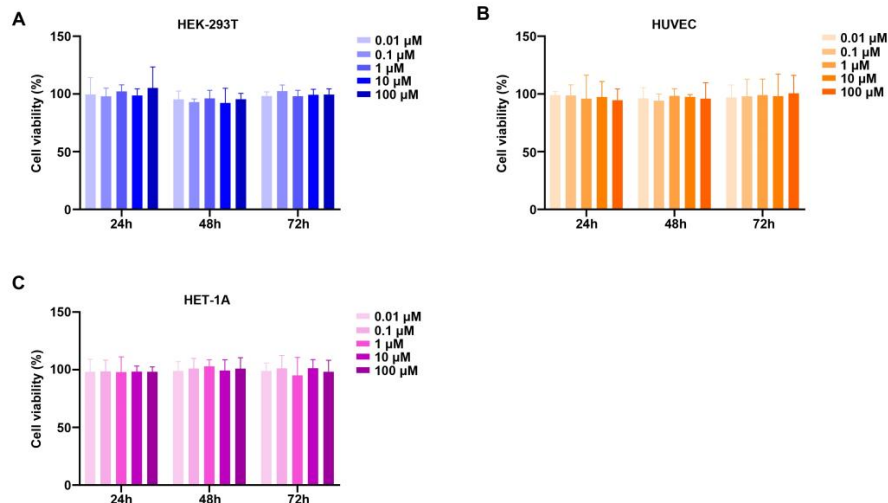
245

246

247







249

250 **Figure S9.** The effect of 3, 5-diiodotyrosine on cell viability. (A-C) HEK-293T,

251 HUVEC and HET-1A cells were treated with different concentrations of 3,

252 5-diiodotyrosine for 24, 48 and 72 hours, and cell viability was measured by MTT

253 analysis. Data are representative of at least three independent experiments.

254

255

256

257

258

259

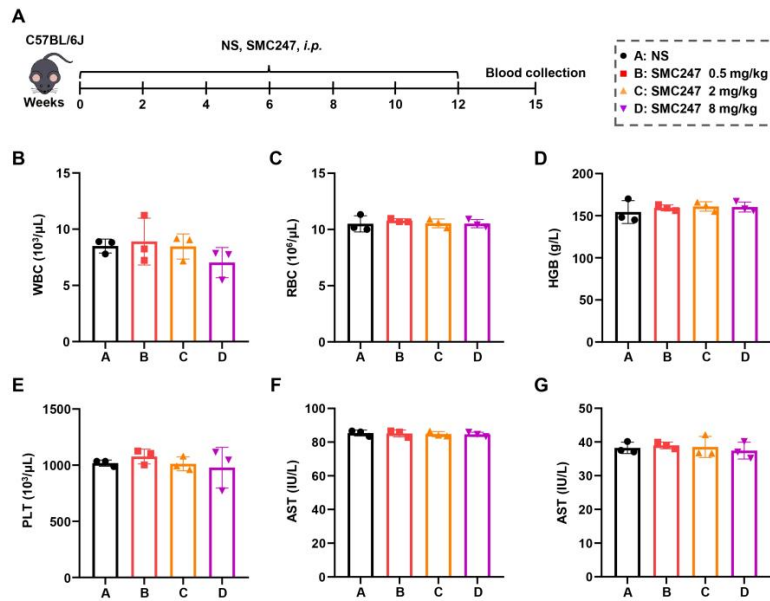
260

261

262

263

264



265

266 **Figure S10.** Toxicity evaluation of 3, 5-diiodotyrosine *in vivo*. (A) Seven-week-old  
 267 naive female C57BL/6J mice were *i.p.* injected with 200  $\mu\text{L}$  normal saline and  
 268 different dosages of 3, 5-diiodotyrosine (0.5 mg/kg, 2 mg/kg, and 8 mg/kg),  
 269 respectively, every two days for 7 times. (B-E) Blood physiology indexes (WBC,  
 270 RBC, HGB and PLT) of mice were analyzed by blood routine assay. (F, G)  
 271 Biochemistry indexes of mice (AST and ALT) were analyzed by AST and ALT kit,  
 272 respectively (n = 3).

273

274

275

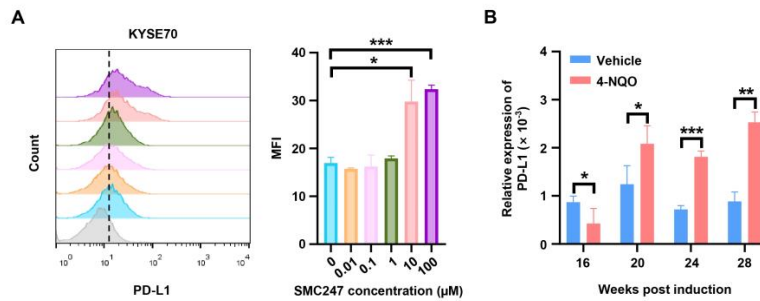
276

277

278

279

280



281

282 **Figure S11.** The expression level of PD-L1 in ESCC cell line and tumor tissue. (A)

283 The expression of PD-L1 in KYSE70 cell after treatment with different concentrations

284 (0, 0.01, 0.1, 1, 10, 100  $\mu\text{M}$ ) of 3, 5-diiodotyrosine for 48 hours was measured by

285 flow cytometry. (B) The mRNA expression of PD-L1 in esophageal tissues of vehicle

286 mice and 4-NQO induced ESCC mice at different periods was detected by qRT-PCR

287 ( $*P < 0.05$ ,  $**P < 0.01$ ,  $***P < 0.001$ ).

288

289

290

291

292

293

294

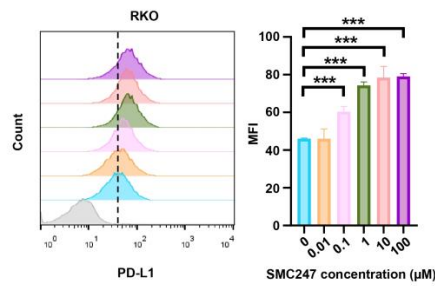
295

296

297

298





300

301 **Figure S12.** The expression of PD-L1 in colon cancer cell line. Flow cytometry  
302 analysis of PD-L1 expression in RKO cell after treatment with different  
303 concentrations (0, 0.01, 0.1, 1, 10, 100 μM) of 3, 5-diiodotyrosine for 48 hours. The  
304 statistical analysis was conducted by one-tailed Student's *t* test (\*\*\*)  $P < 0.001$ .

305

306

307

308

309

310

311

312

313

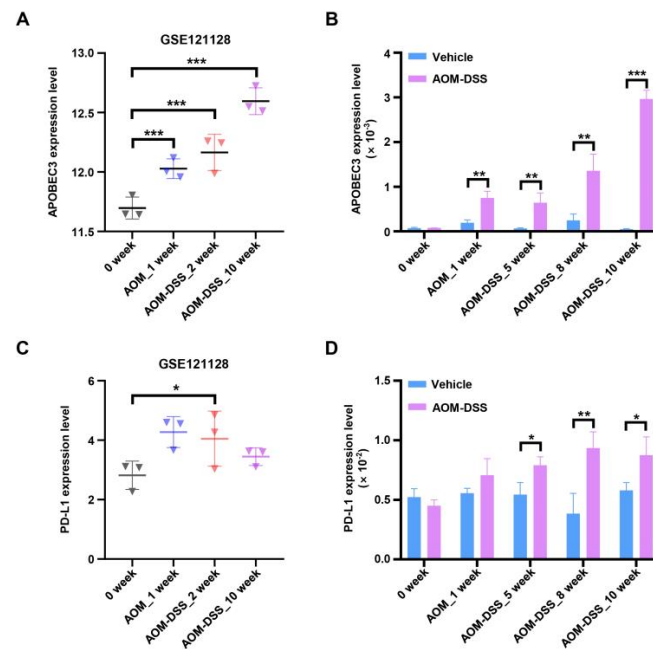
314

315

316

317

318



319

320 **Figure S13.** The expression levels of APOBEC3 and PD-L1 in colon tissues of

321 vehicle mice and AOM/DSS induced colon cancer mice at different periods. (A, C)

322 The expression levels of APOBEC3 and PD-L1 in colon tissues at 0, 1, 2 and 10

323 weeks after AOM/DSS induction were analyzed from GEO database (GSE121128) (n

324 = 3). (B, D) The expression levels of APOBEC3 and PD-L1 in colon tissues of AOM

325 / DSS induced colon cancer mice and vehicle at different time points (0, 1, 5, 8, 10

326 weeks) were analyzed (n = 3, \* $P < 0.05$ , \*\* $P < 0.01$ , \*\*\* $P < 0.001$ ).

327

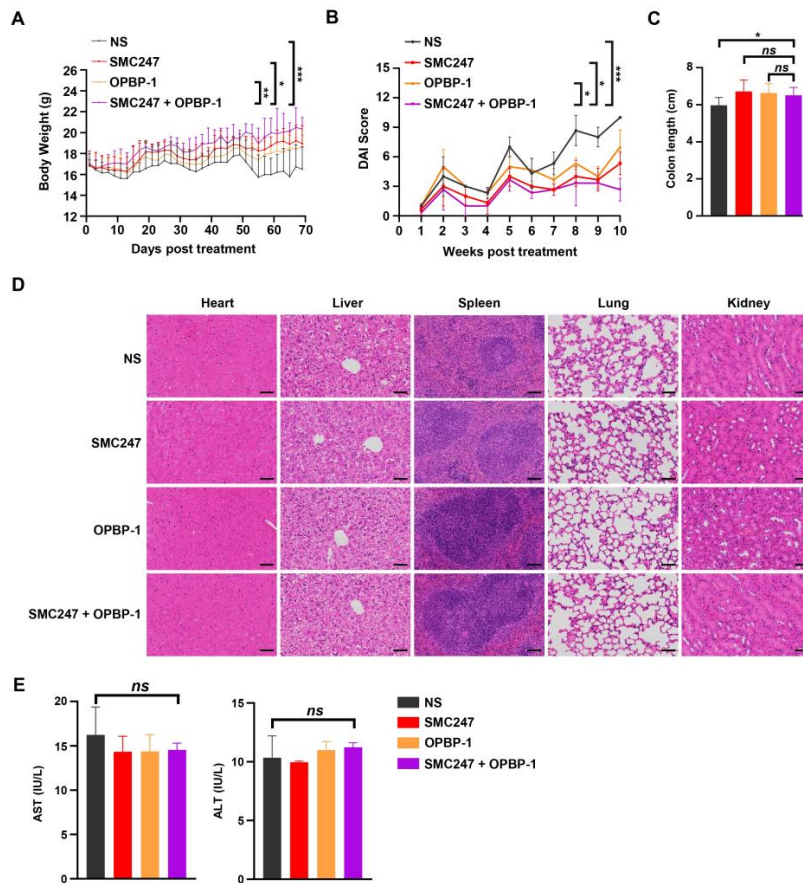
328

329

330

331

332



333

334 **Figure S14.** Model establishment of colon cancer mice induced by AOM/DSS and

335 changes of physiological indexes after 3, 5-diiodotyrosine combined with OPBP-1

336 treatment. (A-B) The changes of body weight and DAI score in each group (n = 6 or

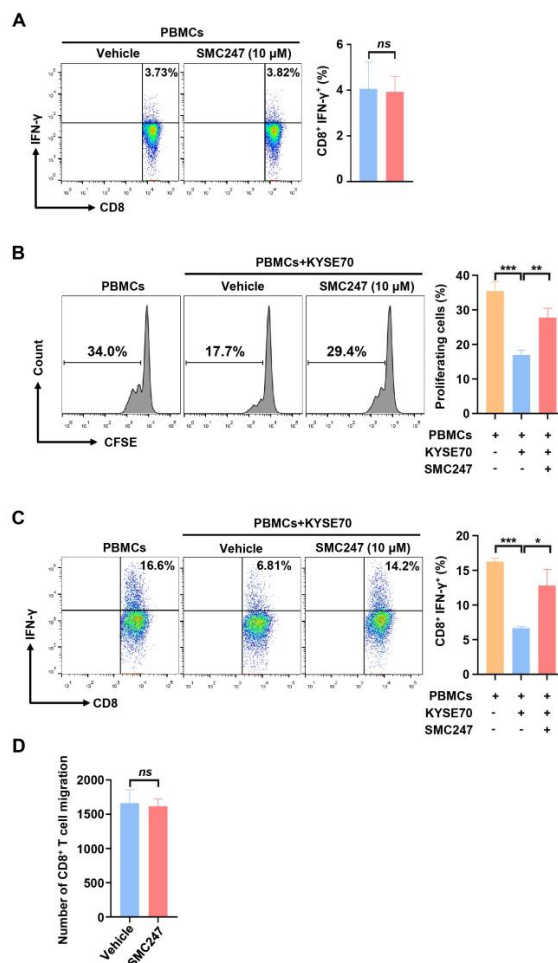
337 7, \* $P < 0.05$ , \*\* $P < 0.01$ , \*\*\* $P < 0.001$ ). (C) Colon length in each group. (D) The338 H&E staining of mice organs in each group after treatment (Scale bars: 100  $\mu\text{m}$  for339 heart, liver, lung and kidney, 50  $\mu\text{m}$  for spleen). (E) Analysis of hepatic damage by the

340 level of AST and ALT in serum (n = 3).

341

342

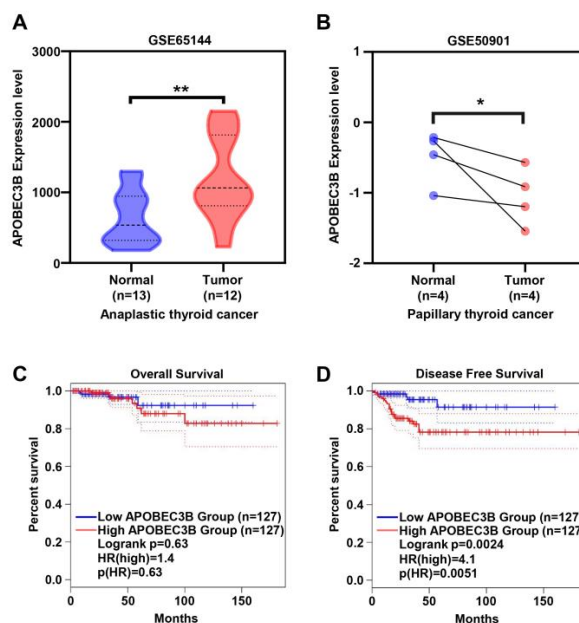
343



344

345 **Figure S15.** The effect of 3, 5-diiodotyrosine on CD8<sup>+</sup> T cell function. (A) PBMCs  
 346 were isolated and activated with 100 units IL-2, 1  $\mu$ g/mL anti-CD3, and 1  $\mu$ g/mL  
 347 anti-CD28 stimulatory antibodies and directly treated with 10  $\mu$ M 3, 5-diiodotyrosine  
 348 for 3 days. Then proportion of IFN- $\gamma$ <sup>+</sup>CD8<sup>+</sup> T cells were analyzed by flow cytometry.  
 349 (B, C) Activated PBMCs were cocultured with KYSE70 cells within the addition of  
 350 10  $\mu$ M 3, 5-diiodotyrosine. The proliferation of CD8<sup>+</sup> T cells and proportion of  
 351 IFN- $\gamma$ <sup>+</sup>CD8<sup>+</sup> T cells were analyzed by flow cytometry. (D) The migration number of  
 352 CD8<sup>+</sup> T cells was analyzed by flow cytometry. Data are representative of at least three  
 353 independent experiments (\* $P$  < 0.05, \*\* $P$  < 0.01, \*\*\* $P$  < 0.001).





354

355 **Figure S16.** The expression and prognosis of APOBEC3B in thyroid cancer. (A, B)

356 Expression levels of APOBEC3B in normal and tumor tissues of human anaplastic

357 cancer and papillary thyroid cancer from GEO database were analyzed,  $*P < 0.05$ ,358  $**P < 0.01$ . (C, D) The overall survival curve and disease free survival curve in low

359 expression of APOBEC3B and high expression of APOBEC3B in THCA were

360 analyzed from GEPIA database.

361

362

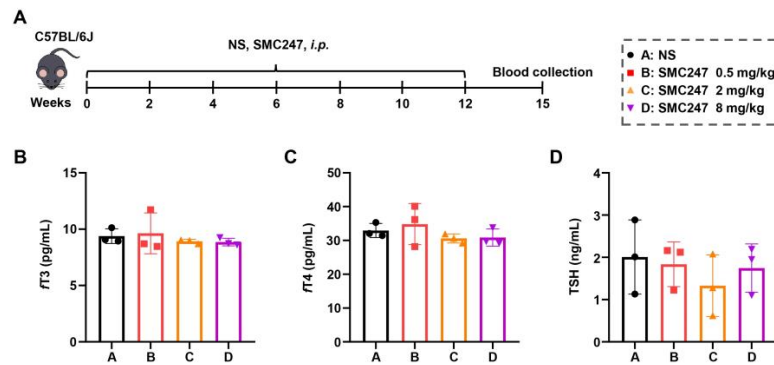
363

364

365

366

367



368

369 **Figure S17.** Effects evaluation of 3, 5-diiodotyrosine on thyroid function *in vivo*. (A)370 Seven-week-old naive female C57BL/6J mice were *i.p.* injected with 200  $\mu$ L normal

371 saline and different dosages of 3, 5-diiodotyrosine (0.5 mg/kg, 2 mg/kg, and 8 mg/kg),

372 respectively, every 2 days for 2 weeks. (B-D) The main indexes of thyroid function

373 (fT3, fT4 and TSH) in mice were analyzed (n = 3).

374

375

376

377

378

379

380

381

382

383

384

385

386

387

388

389 **Table S1. The primer sequences for qRT-PCR.**

Gene	Species	Forward	Reverse
APOBEC3B	Human	CCATCCTCTATGGTCGGAGC	GAGGCTTGAAATACACCTGGC
IL-7	Human	CCTCCCCTGATCCTTGTTCTG	ACCAATTTCCTTCATGCTGTCCA
IL-15	Human	ACAGAAGCCAACTGGGTGAAT	TGCTGTTACTTTGCAACTGGG
GAPDH	Human	GGAGTCCCTGCCACACTCA	GCCCCTCCCCTCTTCAAG
APOBEC3	Mouse	TGCTACATCTCGGTCCCTTC	TCCTCTTCACTTAGCGGGTC
PD-L1	Mouse	TCACTTGCTACGGGCGTTTAC	AGTTGCTGTGCTGAGGCTTA
GAPDH	Mouse	GCATCCACTGGTGCTGCC	TCATCATACTTGGCAGGTTTC

390

391

392

393

394

395

396

397

398

399

400

401

402

403

404

405

406

407

408

409

410

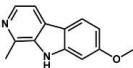
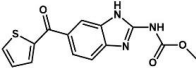
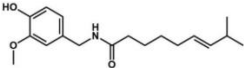
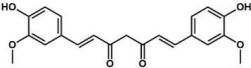
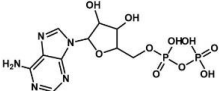
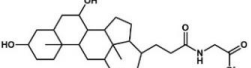
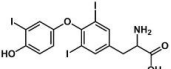
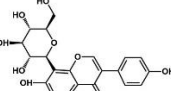
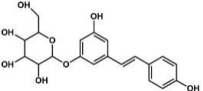
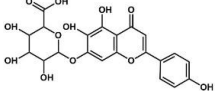
411

412 **Table S2. Specific information for the crystal structures of human APOBEC3B.**

NO.	PDBID	Notation	Resolution (Å)	Length	Mutation and missing	Reference
1	2NBQ	monomer	-	187-378	-	Biochemistry, 2016
2	5CQD	monomer	2.08	187-378	F200S, W228S, L230K, Y250S, F308K; Missing: A242-F249	J Biol Chem, 2015
3	5CQH	monomer	1.73	187-378	F200S, W228S, L230K, Y250S, F308K; Missing: A242-F249	J Biol Chem, 2015
4	5CQI	monomer	1.68	187-378	F200S, W228S, L230K, Y250S, F308K; Missing: A242-F249	J Biol Chem, 2015
5	5CQK	monomer	1.88	187-378	F200S, W228S, L230K, Y250S, F308K	J Biol Chem, 2015
6	5SXG	monomer	1.93	191-378	F200S, W228S, L230K, Y250S, F308K; Missing: D224-M231, A242-F249	Sci Rep, 2017
7	5SXH	monomer	1.78	191-378	L230K, Y250S, F308K; Missing: N225-M231, A242-F249	Sci Rep, 2017
8	5TD5	<b>APOBEC3B-ssD NA complex</b>	<b>1.72</b>	<b>191-378</b>	<b>F200S, D205G, R212H, Q213K, W228S, L230K, R210G, L209I, Y250S, E255A, F308K; missing: P206-V208, A242-F249</b>	<b>Nat Struct Mol Biol, 2017</b>
9	5TKM	monomer	1.90	1-191	Y83D, W127S, Y162D	Nucleic Acids Res, 2017
10	6NFK	monomer	1.86	187-378	F200S, W288S, L230K, Y250S, E255Q, F308K, Y315D, D316Q, P317G, L318R, Y319C, K320Q; Missing: A242-F249	FASEB Bioadv, 2019
11	6NFL	monomer	1.73	187-378	F200S, W288S, L230K, Y250S, F308K, Y315D, D316Q, P317G, L318R, Y319C, K320Q; Missing: A242-F249	FASEB Bioadv, 2019
12	6NFM	monomer	2.53	187-378	F200S, W288S, L230K, Y250S, F308K, Y315D, D316Q, P317G, L318R, Y319C, K320Q; Missing: A242-F249	FASEB Bioadv, 2019

413

414 **Table S3. Structure and inhibition rate of 10 hit compounds in enzyme assay.**

Compounds	Mol ID	2D structure	S score	Molecule weight	Log (O/W)	RMSD (Å)	Inhibition rate (%)
SMC111	T1711		-5.47	212.25	2.92	3.35	53.64
SMC115	T2802		-6.45	301.33	2.31	1.27	25.94
SMC116	T1062		-6.76	305.42	3.56	1.99	32.27
SMC118	T1516		-7.07	368.40	3.72	1.53	75.23
SMC121	T1723		-6.87	427.20	-4.09	1.34	41.76
SMC123	T2831		-7.11	464.62	3.15	2.08	23.67
SMC130	T1653		-5.54	650.98	3.45	2.09	70.19
SMC132	T2815		-7.45	416.38	-0.3	1.95	37.51
SMC139	T3427		-7.16	390.39	1.43	1.97	31.47
SMC140	T3242		-7.48	462.36	0.47	1.56	41.25

415 Inhibition rate indicates that the inhibition effect of compounds on APOBEC3B

416 activity at the concentration of 100  $\mu$ M.

417 S score indicates the comprehensive score for docking minimum energy.

418

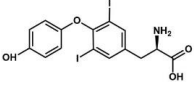
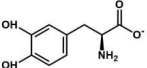
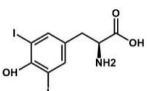
419

420

421

422

423 **Table S4. Representative 2D similarity searching results and docking results of**  
424 **SMC130.**

Compounds	Mol ID	2D structure	Molecular name	S score	Molecule weight	RMSD (Å)	Similarity score
SMC245	T4461		3,5-Diiodo-L-tyrosine	-7.70	525.08	2.76	0.95
SMC246	T0848		Levodopa	-8.97	197.19	2.00	0.70
SMC247	T2760		3,5-Diiodotyrosine	-9.08	432.98	0.91	0.79

425

426

427

428

429

430

431

432

433

434

435

436

437

438

439

440

441

442

443

444

445 **Table S5. The ssDNA sequences in fluorescence-based single-stranded DNA**  
446 **cytosine deamination assay.**

Gene	Sequence
APOBEC3A	5'-6-FAM-ATTATTATTATTCTAATGGATTATTTATTTATTTATTTATTTATTT-TAMRA-3'
APOBEC3B	5'-6-FAM-ATTATTATTATTCAAATGGATTATTTATTTATTTATTTATTTATTT-TAMRA-3'
APOBEC3G	5'-6-FAM-ATTATTATTATTCCAATGGATTATTTATTTATTTATTTATTTATTT-TAMRA-3'

447

448

449

450

451

452

453

454

455

456

457

458

459

460

461

462

463

464

465

466

467

468

469

470

471 **Table S6. The detailed DAI scoring criteria.**

Score	Range of body weight loss	Stool appearance	Hematochezia
0	None	Normal	Normal
1	1-5%	—	—
2	5-10%	Light diarrhoea	—
3	10-20%	—	—
4	>20%	Severe diarrhoea	Severe hematochezia

472

473